The ROYAL COLLEGE of
OPHTHALMOLOGISTS

ARTICLE

Mesopic and dark-adapted two-color fundus-controlled perimetry in patients with cuticular, reticular, and soft drusen

Maximilian Pfau[1] · Moritz Lindner [1,2] · Martin Gliem[1] · Julia S. Steinberg[1] · Sarah Thiele[1] · Robert P. Finger[1] · Monika Fleckenstein[1] · Frank G. Holz[1] · Steffen Schmitz-Valckenberg[1]

Abstract

Purpose To examine the feasibility and utility of dark-adapted two-color fundus-controlled perimetry (FCP) in patients with cuticular, reticular, and soft drusen, and to compare FCP data to microstructural spectral-domain optical coherence tomography (SD-OCT) data.

Methods Forty-four eyes (24 eyes of 24 patients with drusen, age 69.4 ± 12.6 years; 20 normal eyes of 16 subjects, 61.7 ± 12.4 years) underwent duplicate mesopic, dark-adapted cyan and dark-adapted red FCP within $14°$ of the central retina (total of 12 936 threshold tests) using the Scotopic Macular Integrity Assessment (S-MAIA, CenterVue, Padova, Italy) device. FCP data were registered to SD-OCT data to obtain outer nuclear layer, inner and outer photoreceptor segment, and retinal pigment epithelium drusen complex (RPEDC) thickness data spatially corresponding to the stimulus location and area ($0.43°$). Structure-function correlations were assessed using mixed-effects models.

Results Mean deviation values for eyes with cuticular, soft, and reticular drusen were similar for mesopic (-2.1, -3.4, and -3.6 dB) and dark-adapted red (-1.4, -2.6, and -3.3 dB) FCP. For the dark-adapted cyan FCP (0.1, -1.9, and -5.0 dB) and for the cyan–red sensitivity difference ($+1.0$, $+0.5$, and -2.4 dB), the mean deviation values differed significantly in dependence of the predominant drusen type (one-way ANOVA; $p < 0.05$). RPEDC thickness was associated with reduction of mesopic sensitivity (-0.34 dB/10 µm RPEDC thickening; $p < 0.001$), dark-adapted cyan sensitivity (-0.11 dB/10 µm RPEDC thickening; $p = 0.003$), and dark-adapted red sensitivity (-0.26 dB/10 µm RPEDC thickening; $p < 0.001$).

Conclusions In contrast to mesopic FCP, dark-adapted two-color FCP allowed for meaningful differential testing of rod and cone function in patients with drusen indicating predominant cone dysfunction in eyes with cuticular drusen and predominant rod dysfunction in eyes with reticular drusen. RPEDC thickness was the strongest predictor of the evaluated SD-OCT biomarkers for point-wise sensitivity.

✉ Steffen Schmitz-Valckenberg
steffen.schmitz-valckenberg@ukbonn.de

1 Department of Ophthalmology, University of Bonn, Ernst-Abbe-Str. 2, Bonn, Germany

2 The Nuffield Laboratory of Ophthalmology, Sleep and Circadian Neuroscience Institute, Nuffield Department of Clinical Neurosciences, University of Oxford, Oxford, UK

Introduction

Late-stage age-related macular degeneration (AMD) is the leading cause of visual impairment in developed countries [1]. Currently, no therapy is available for the non-exudative late-stage manifestation of AMD termed geographic atrophy [2]. Moreover, long-term results of anti-vascular endothelial growth factor treatment for the exudative late-stage manifestation (choroidal neovascularization) are limited, since a significant proportion of patients progresses to severe visual impairment over time despite of treatment [3]. Thus, there is an unmet need for therapeutic strategies that prevent conversion from early AMD to both of the late-stage manifestations [1].

SPRINGER NATURE

However, clinical trials in the setting of intermediate AMD constitute a challenge due to the lack of validated structural and functional surrogate end points beyond conversion to late AMD [4]. Best-corrected visual acuity (BCVA) is inappropriate since it is normal or only minimally impaired in most patients [5]. Prompted by histological findings indicating that rod loss may exceed cone loss in eyes with AMD, previous studies have focused on probing rod function [6]. These include dark-adapted perimetry [7, 8], two-color dark-adapted perimetry [9], and rod-mediated dark adaptation [10–13]. Yet, all of the aforementioned functional tests are not fundus-controlled limiting the accuracy of structure-function correlation. So far, one other study has probed dark-adapted thresholds under scotopic conditions in patients with AMD and reticular drusen using fundus-controlled perimetry (FCP) for precise structure-function correlation [8, 14]. Recently, a modified version of the Macular Integrity Assessment (MAIA, CenterVue, Padova, Italy) device with two additional projection light-emitting diodes has become available. It allows for mesopic testing (background $1.27 \, cd/m^2$) FCP with achromatic stimuli as well as two-color dark-adapted FCP with cyan (505 nm) and/or red (627 nm) stimuli [15–18].

Structural biomarkers in intermediate AMD have been assessed by color fundus photography, volumetric spectral-domain optical coherence tomography (SD-OCT) data, qualitative SD-OCT data, and fundus autofluorescence [4]. In terms of structure-function correlation with quantitative SD-OCT data, retinal pigment epithelium + drusen complex (RPEDC) thickness, drusen thickness, and outer retina thickness have been shown to be associated with photopic (standard automated perimetry) sensitivity, rod-mediated dark adaptation as well as mesopic FCP sensitivity [19–25]. In the setting of reticular drusen, partial outer retinal volume (outer nuclear layer (ONL) and inner segments) was shown to be markedly associated with dark-adapted sensitivity using FCP [8, 14].

Multiple drusen phenotypes, which represent the hallmark finding in early and intermediate AMD, have been distinguished, including soft drusen, cuticular drusen, and reticular drusen (subretinal drusenoid deposits) [26]. While dyschromatopsia as well as reduction of photopic and mesopic sensitivity have been previously reported for patients with cuticular drusen (in presence of central vitelliform lesions), subjective night blindness or rod dysfunction have not been reported for patients with cuticular drusen [27, 28]. In contrast multiple studies have described rod dysfunction in patients with soft drusen (cf. above) and most notably for eyes with reticular drusen [8, 12, 14, 19, 29–32].

The present work examines the feasibility and utility of dark-adapted two-color FCP with the Scotopic-MAIA (S-MAIA) device in patients with cuticular, soft, and reticular drusen as compared to age-matched normal eyes.

Based on previous psychophysical studies, we hypothesized that dark-adapted two-color FCP would allow for differential functional phenotyping of eyes with cuticular drusen (predominant cone dysfunction), soft drusen (cone and rod dysfunction), and reticular drusen (predominant rod dysfunction). Effect sizes of SD-OCT structural biomarkers on mesopic and dark-adapted cyan and red sensitivity were compared as a prerequisite for clinical trial design.

Methods

Subjects

To be included at least one eye of the subjects had to show cuticular drusen, reticular drusen, or signs of intermediate AMD (large drusen [≥125 µm] or pigmentary abnormalities associated with at least medium drusen [≥63–<125 µm]) [33]. All patients were recruited at the Department of Ophthalmology, University of Bonn, Germany. Exclusion criteria were refractive errors ≥ 5.00 D of spherical equivalent and >1.50 D of astigmatism assessed by autorefraction (ARK-560A, Nidek, Gamagori, Japan) as well as a history of glaucoma or relevant anterior segment diseases with media opacity, including cataract. Eyes with blue-light-filtering intraocular lenses were not included in this study. If both eyes met the inclusion criteria, the eye with better visual acuity was included. All subjects underwent routine ophthalmological examinations, including BCVA, slit-lamp, and funduscopic examinations. SD-OCT raster scanning was performed using a $30° \times 25°$ scan field (121 B-scans, automated real-time mode 20 frames, centered on the fovea, Spectralis OCT2, Heidelberg Engineering, Heidelberg, Germany). The study was approved by the Institutional Review Board of the University of Bonn (ethics approval ID: 191/16). After explanation of the nature and possible consequences of the study, informed written consent was obtained from all subjects. The protocol followed the tenets of the Declaration of Helsinki.

Normal controls

A dataset of 20 normal eyes of 16 subjects (mean age 61.7 ± 12.4 years, 10 females) with duplicate mesopic, dark-adapted cyan, and dark-adapted red FCP (total of 5880 threshold tests) was used as a comparator [15]. The hierarchical nature of the data (stimulus position nested in eye nested in patient) was taken into account using mixed-effects models [34]. SD-OCT data were obtained from 21 subjects in normal retinal health (mean age 71.5 ± 11.3 years, 15 females). These eyes have been previously included in a point-wise retest-reliability analysis [15]. As dense SD-OCT scans were not available for all normal subjects that

underwent duplicate FCP, the cohorts for the normative SD-OCT and FCP data are not identical but overlap.

Fundus-controlled perimetry

A short mesopic practice examination was performed in patients with no prior perimetry or FCP experience. Following pupil dilation with 1.0% tropicamide, all patients underwent duplicate mesopic (achromatic stimuli, 400–800 nm) FCP, followed by 30 min of dark adaption (light level < 0.1 lux) and then duplicate DA cyan (505 nm) and duplicate DA red (627 nm) FCP. All tests were carried out using a grid of 49 stimuli covering 14° of the central retina with the S-MAIA. Mesopic testing was performed with the preset 4–2 dB staircase strategy, while DA testing was performed with the preset 2–1 dB staircase strategy. The stimulus size was 0.43° (Goldmann III). The exact test algorithm has been described previously in detail [16].

Image analysis and grading

Volumetric SD-OCT data were automatically segmented as implemented in the manufacturer's software (Spectralis Viewing Module 6.3.2.0, Heidelberg Engineering, Heidelberg, Germany). Thereafter, the segmentation was reviewed and—if indicated—manually corrected by two consecutive readers. We defined all layers between the internal limiting membrane (ILM) and the boundary of the outer plexiform layer and ONL as inner retina [35]. In analogy to Sadigh et al. [36], the Henle fiber layer (HFL) was counted towards the ONL. The inner and outer photoreceptor segment (IS + OS) thickness ranged from band 1 (ELM) to band 3 (putative interdigitation zone) [35]. The RPEDC ranged from band 3 to Bruch's membrane. As defined by Chiu et al. [37], the RPEDC encompassed all drusen material, whether below the RPE (soft drusen and cuticular drusen) or above the RPE (reticular drusen, vitelliform debris). The thickness from ILM to Bruch's membrane was defined as full retinal thickness. Further, the eyes of the patients were classified according to the predominant drusen type in analogy to Gliem et al. [38]. The specific criteria are listed in Table S1 (Fig. 1) [38].

Volumetric thickness maps for each layer were transferred as tab-delimited file to ImageJ (U.S. National Institutes of Health, Bethesda, MD, USA) together with an outer retinal en-face image (mean intensity projection, 50 μm thick slab centered on IS/OS). To account for eye tilt and eye rotation between the FCP and SD-OCT examinations, the FCP data were registered to the outer retinal en-face image using the moving least squares (nonlinear) method (alpha 1.0, mesh resolution 32, affine transformation) as implemented in ImageJ (Fig. 2). The mean thickness values of the volumetric SD-OCT data topographically corresponding to the stimuli locations and area (diameter of 0.43°) were extracted using the measure function of ImageJ (Fig. 2).

Outcome measures and statistical analyses

Statistical analyses were performed using the software environment R and the package nlme [39]. Visual acuity measurements (Snellen fractions) were converted to the base-10 logarithm of the minimum angle of resolution (logMAR) [40]. The mean deviation (MD), corrected pattern standard deviation (cPSD), and short-term fluctuation were calculated according to Heijl et al. [41]. Cumulative defect curves (Bebie curves) were plotted to allow for graphical separation of focal and global components of visual field deficit [42]. The MD was compared for each type of testing among the types of drusen using analyses of variance (ANOVAs) followed by Tukey's honestly significant difference test.

For the retinotopic structure-function correlation, both the FCP and SD-OCT normative data were standardized (z-scores) to fully account for the retinotopic dependence of mean values and inter-individual variability. In a first step, predictor variables were identified that showed a significant effect on sensitivity by constructing mixed-effects models for each SD-OCT biomarker separately. The mixed-effects models took into account the hierarchical structure of the data (stimulus location nested in eye) and included the results of both, the test and retest. Last, a mixed-effects model with all of the previous significant predictors was constructed to compare the effect sizes of the biomarkers.

Results

Cohort characteristics

Perimetry data of 24 eyes with intermediate AMD (24 patients, age [mean ± SD] 69.4 ± 12.6 years, range 48.3–90.1 years, 16 female) with duplicate mesopic, dark-adapted cyan, and dark-adapted red FCP were included in the analysis. The average BCVA was 0.07 ± 0.09 logMAR (Snellen equivalent approximately 20/25). For every patient, the MD and cPSD visual field indices were computed. Further, the patients were classified according to their predominant drusen type as shown for three exemplary cases in Fig. 1 (see also Table 1).

Retest variability

The short-term fluctuation as indicator of retest variability was low in eyes with intermediate AMD for all three types of testing with values (mean [range]) of 1.99 dB (1.4–2.94 dB) for mesopic, 1.91 dB (1.28–3.36 dB) for dark-adapted
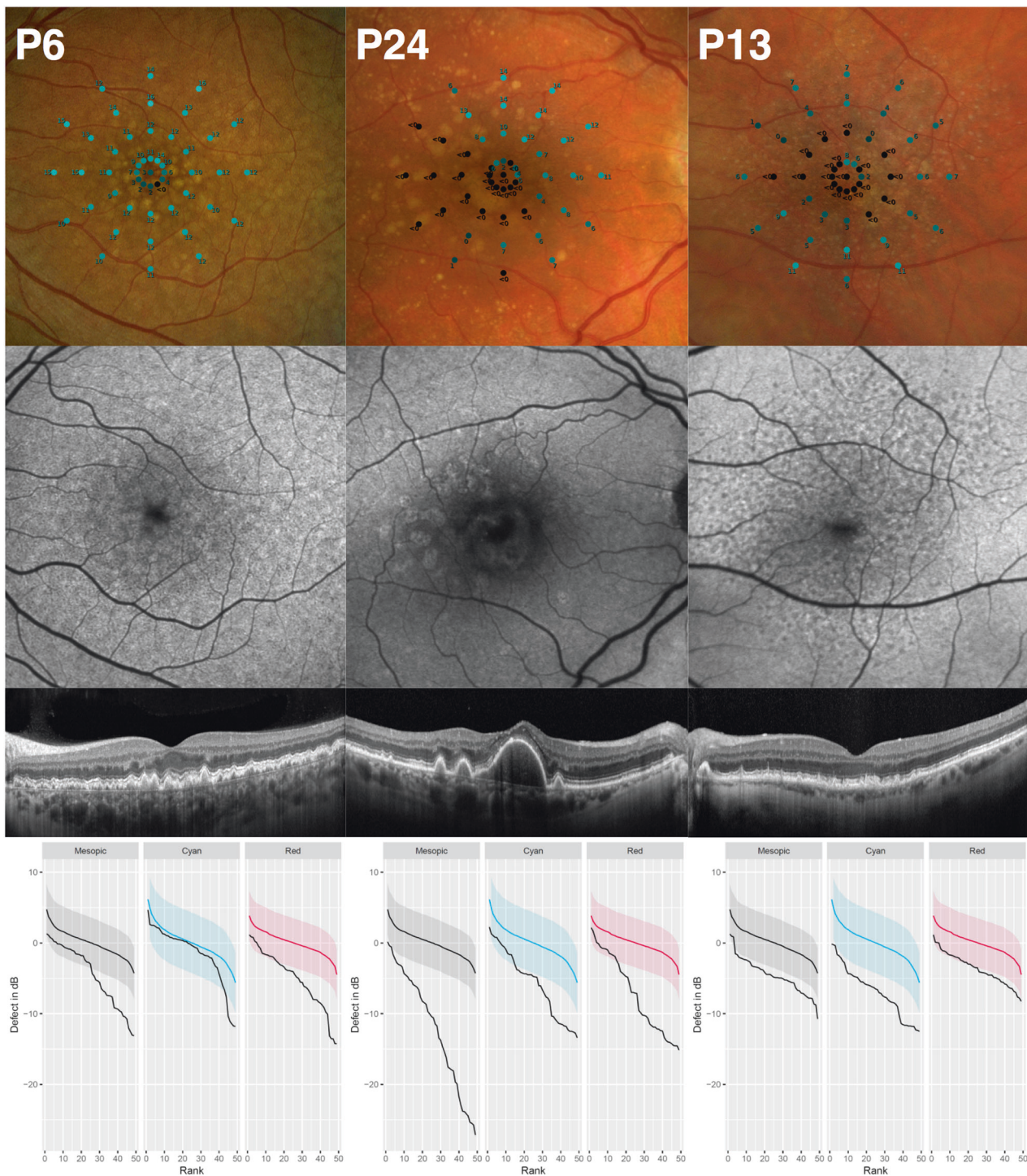
Fig. 1 The columns show a representative example eye for each drusen type (from left to right) with color fundus photography (first row), fundus autofluorescence imaging (second row), and the horizontal spectral-domain optical coherence tomography B-scan centered to the fovea (third row). The overlay in the color fundus photographs displays the results of the first dark-adapted cyan test. The last row depicts the corresponding cumulative defect (Bebie) curves for each type of testing. The normative data with 95% confidence intervals are shown in the background. The data of the patient are plotted in the foreground. Patient 6 (P6) exhibited multiple, yellowish, small, round, "hard" drusen with distinct borders and was classified as predominant cuticular drusen. The cumulative defect curves indicated that the mesopic and dark-adapted red deficit exceeded the dark-adapted cyan deficit. Patient 24 (P24) exhibited multiple confluent "soft" drusen and was thus classified as predominant soft drusen. The cumulative defect curves indicated defect for all three types of testing. Patient 13 (P13) exhibited small dot- and ribbon-shaped lesion and was classified as predominant reticular drusen. The cumulative defect curves exhibited parallel shift for mesopic and dark-adapted red testing along the y-axis (indicating global defect or media opacity) and most prominently global and diffuse defect for dark-adapted cyan testing
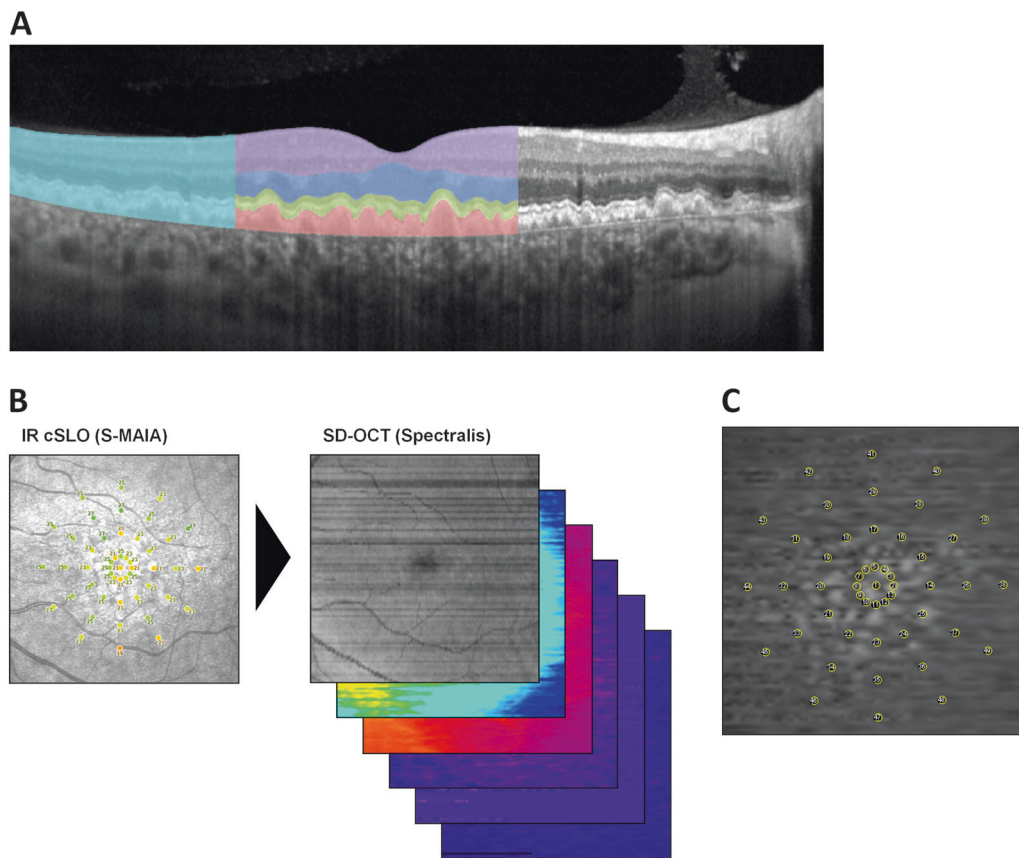
Fig. 2 The spectral-domain optical coherence tomography (SD-OCT) data were segmented semi-automatically (internal limiting membrane [ILM], outer plexiform layer and outer nuclear layer boundary [OPL/ONL], external limiting membrane [ELM], interdigitation zone [IZ], and Bruch's membrane [BM]). The retinal pigment epithelium drusen complex (RPEDC) ranged from BM to the IZ (red overlay). The inner and outer segments (IS + OS) ranged from the IZ to the ELM (green overlay). The ONL ranged from the ELM to the OPL/ONL boundary (blue overlay). Hereby, the Henle fiber layer was counted toward the outer nuclear layer as shown in **a**. The inner retina encompassed all layers from the OPL/ONL boundary to the ILM (purple overlay). The full retina was defined as thickness from BM to the ILM (turquoise overlay). The fundus-controlled perimetry grid consisted of 49 test points over 14° of the central retina as shown in **b** (central test point plus 12 test points at an eccentricity of 1°, 3°, 5°, and 7°). The FCP data were registered to an SD-OCT en-face image using nonlinear affine transformation according to vessel bifurcations. Thus, the FCP data were also aligned to the thickness maps of the corresponding layers (**b**). Thickness data corresponding to the precise stimulus location and area (Goldmann III, 0.43°) was then extracted from the SD-OCT data for each layer (**c**)

cyan, and 1.61 dB (1.1–2.86 dB) for dark-adapted red testing. The short-term fluctuation values did not differ from the short-term fluctuation values in normal eyes for mesopic (1.8 dB [1.22–2.51 dB]), dark-adapted cyan (1.92 dB [1.24–3.64 dB]), and dark-adapted red (1.52 dB [1.09–2.51 dB]) testing (*t*-test, $p = 0.08$, 0.94, and 0.37, respectively).

Differences in visual field indices

For mesopic testing, eyes with cuticular (average MD of −2.1 dB), soft (−3.4 dB), and reticular drusen (−3.6 dB) exhibited similar MD values (one-way ANOVA, $p = 0.613$). Similarly, there were no significant differences for the dark-adapted red MD values (−1.4 versus −2.6 versus −3.3 dB; $p = 0.32$). For dark-adapted cyan testing, the MD values differed significantly in dependence of drusen type ($p = 0.00264$). Post hoc comparisons using the Tukey honestly significant difference test indicated that the mean MD value for reticular drusen (−5.0 dB) was significantly lower as compared to cuticular (+0.1 dB, $p = 0.0019$) drusen and (not significantly) lower as compared to soft drusen (−1.9 dB, $p = 0.053$). Likewise, the MD value for the cyan–red sensitivity difference was significantly associated with the drusen type ($p = 0.001$). It was significantly lower for reticular drusen (−2.4 dB) as compared to both, cuticular (+1.0 dB, $p = 0.001$) and soft (+0.5 dB, $p = 0.004$) drusen. Evaluating the three functional tests and the cyan–red difference in dependence of eccentricity (Fig. 3), a similar degree of mesopic and dark-adapted red MD was observed at 0–1° and 3° for cuticular drusen (Fig. 3). As only subtle differences for the

**Table 1** Patient characteristics

Patient	Age	Drusen type	BCVA (logMAR)	Lens status	Mesopic MD (dB)	Mesopic cPSD (dB)	Cyan MD (dB)	Cyan cPSD (dB)	Red MD (dB)	Red cPSD (dB)	Cyan–red difference MD (dB)	Cyan–red difference cPSD (dB)
P1	49.5	Cuticular	0	Phakic	1.22	1.86	3.06	1.17	1.81	1.84	0.95	1.82
P2	53.7	Cuticular	0	Phakic	−0.17	1.43	1.86	0.92	0.06	1.19	1.46	2.36
P3	74.2	Cuticular	0.1	Phakic	−0.16	0	1.36	2.12	−0.64	1.07	1.68	1.95
P4	64	Cuticular	0.1	Phakic	−1.62	2.03	0.53	1.35	−0.85	1.91	0.92	0
P5	57	Cuticular	0	Phakic	−0.92	1.83	0.26	2.07	1.83	1.55	−2.03	1.89
P6	48.4	Cuticular	0	Phakic	−1.18	1.71	0.24	0.81	−1.71	0.34	2.09	0.59
P7	50.6	Cuticular	0	Phakic	−2.49	2.22	0.03	2.53	−1.76	3.37	1.54	2.19
P8	66.3	Cuticular	0.3	Phakic	−4.19	3.95	−1.75	2.87	−5.21	4.09	2.58	2.96
P9	54.6	Cuticular	0.2	Phakic	−9.25	8.3	−4.43	2.6	−5.71	4.61	−0.23	4.07
P10	85.6	Reticular	0.1	PP, Nd:YAG-LCT	−2.97	0	−3.99	2.72	−4.37	1.73	−0.08	2.63
P11	74	Reticular	0	PP, Nd:YAG-LCT	−4.22	1.64	−4.73	3.71	−4.25	2.07	−1.41	3.76
P12	81.6	Reticular	0.1	PP, Nd:YAG-LCT	−2.51	1.42	−4.95	4.05	−1.46	3.33	−4.37	5.31
P13	78	Reticular	0.1	Phakic	−4.56	1.61	−6.4	3.35	−3.08	1.89	−3.7	4.51
P14	77	Soft	0.1	PP	−0.25	2.53	1.25	1.97	−0.36	1.72	1.09	2.62
P15	68.8	Soft	0	PP, Nd:YAG-LCT	1.23	0.99	1.24	2.24	1.7	0	−0.54	1.97
P16	90.1	Soft	0	PP, Nd:YAG-LCT	−2.54	2.51	−0.58	2	−1.47	1.15	1.02	2.29
P17	53.9	Soft	0.1	Phakic	−1.24	0.45	−0.78	0.98	−1.6	1.62	1.33	2.71
P18	78.8	Soft	0.1	Phakic	−1.72	0	−0.91	0.3	−1.54	1.1	0.61	2.29
P19	74.8	Soft	0	PP, Nd:YAG-LCT	−4.32	4.11	−0.91	2.57	−4.56	4.07	2.71	1.75
P20	82.8	Soft	0	PP, Nd:YAG-LCT	−5.31	2.58	−2.85	3.52	−3.74	2.91	0.32	2.74
P21	72	Soft	0	Phakic	−2.55	3.27	−3.2	2.22	−3.21	2.78	0.08	3.09
P22	77.3	Soft	0.1	Phakic	−3.14	3.33	−3.22	2.62	−3.71	2.27	−0.08	1.79
P23	69.5	Soft	0	Phakic	−4.45	3.01	−3.82	5.53	−3.41	2.76	−1.15	4.9
P24	83.2	Soft	0.3	PP, Nd:YAG-LCT	−12.56	8.12	−6.83	5.5	−6.17	4.86	0.05	3.23
Summary (Mean ± SD)		Cuticular	0.08 ± 0.11		−2.08 ± 3.09	2.59 ± 2.37	0.13 ± 2.17	1.83 ± 0.78	−1.35 ± 2.67	2.22 ± 1.46	1 ± 1.39	1.98 ± 1.19
		Reticular	0.08 ± 0.05		−3.57 ± 0.98	1.17 ± 0.78	−5.02 ± 1.01	3.46 ± 0.57	−3.29 ± 1.35	2.26 ± 0.73	−2.39 ± 1.99	4.05 ± 1.14
		Soft	0.06 ± 0.09		−3.35 ± 3.6	2.81 ± 2.18	−1.87 ± 2.39	2.68 ± 1.63	−2.55 ± 2.17	2.29 ± 1.39	0.49 ± 1.04	2.67 ± 0.89

Test results for each patient included in the study. In addition to age, drusen type, best-corrected visual acuity (BCVA), the mean deviation (MD), and the corrected pattern standard deviation (cPSD) are shown for mesopic thresholds, dark-adapted cyan thresholds, dark-adapted red thresholds as well as the difference between the two latter tests. The cPSD values, which are not influenced by the global defect or optical media and corrected for retest variability (short-term fluctuation), indicated similar trends as compared to the MD values. Eyes with reticular drusen exhibited large cPSD values for dark-adapted cyan testing versus relatively lower cPSD values for dark-adapted red testing. This difference could not be attributed to aging of the crystalline lens. Eyes with blue-light-filtering intraocular lenses were not included in this study

PP pseudophakic, *Nd:YAG-LCT* Nd:YAG laser capsulotomy
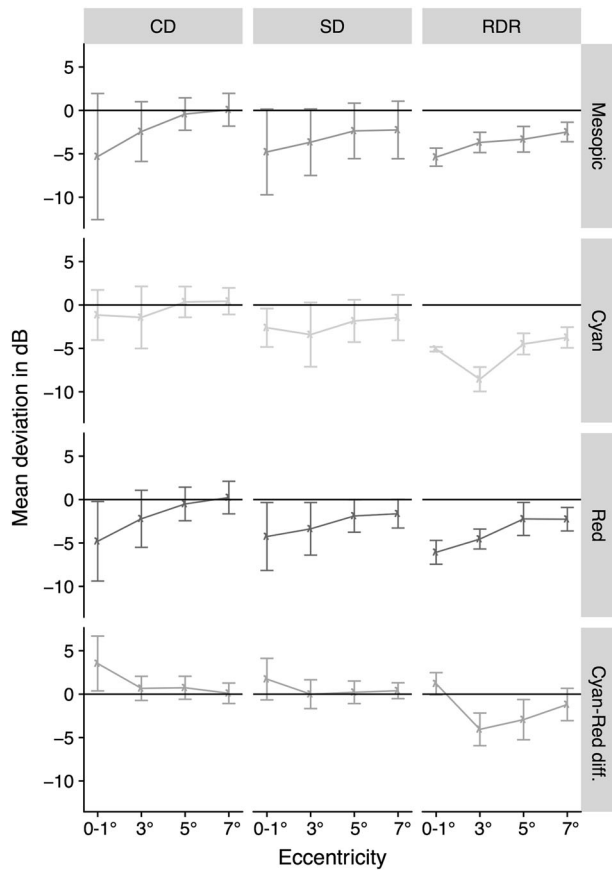
Fig. 3 The plot shows the mean deviation (MD, dots indicate the average MD and error bars the SD of the MD) as compared to normative data of the three functional tests and the cyan–red difference for each predominant drusen type and according to the degree of eccentricity. Eyes with cuticular drusen and soft drusen exhibited high MD for mesopic and dark-adapted red testing at 0–1° with little MD for cyan testing. This resulted in positive values for the MD of the cyan–red sensitivity difference indicating cone dysfunction at 0–1°. At 5° and 7°, eyes with cuticular drusen exhibited overall little MD. Eyes with soft drusen exhibited at 3°, 5°, and 7° equal amounts of MD for dark-adapted cyan and red testing indicating a similar degree of rod and cone dysfunction. Eyes with reticular drusen exhibited at 3°, 5°, and 7° predominantly MD for dark-adapted cyan testing resulting in negative MD values for the cyan–red sensitivity difference, indicating predominant rod dysfunction

dark-adapted cyan threshold as compared to normative data were found, the cyan–red difference for cuticular drusen showed positive MD values at 0–1° and 3° indicating cone dysfunction. Eyes with soft drusen exhibited similar amounts of MD values across all three types of testing across all eccentricities, indicating a similar degree of cone and rod dysfunction. For eyes with reticular drusen the dark-adapted cyan MD exceeded the dark-adapted red MD markedly at 3°–7°, indicating predominant rod dysfunction.

The cPSD disclosed similar results as compared to the MD values (Table 1).

Retinotopic structure-function correlation

The inter-individual variability of both FCP and SD-OCT data varied in dependence of the retinal location. For instance, with regard to dark-adapted red testing, a deviation of 5 dB at 7° for a given stimulus point would exceed the 95% confidence interval ($CI = 1.96 \times SD_{7° \, red}$, Table S2), while the same amount of deviation at 0–1° would still be within the 95% CI. Likewise, ONL thinning by more than $-24 \, \mu m$ at 7° would be outside of the 95% CI, while the same amount of ONL thinning would still be within the 95% CI at 0–1° (Table S2). Thus, all of the following analyses were performed using the number of normative SDs from the normative mean (i.e., z-scores, Table S2) for both, the FCP as outcome variable and the SD-OCT data as explanatory variable.

Linear mixed-effects models, considering each point-wise SD-OCT biomarker separately together with the predominant drusen type, disclosed that for all three types of testing that point-wise full retinal thickness, ONL thickness, and RPEDC thickness were significantly associated with the point-wise sensitivity (Table S3). Point-wise inner retinal thickness had no influence on all three types of testing. Point-wise IS + OS thickness had no influence on point-wise dark-adapted cyan ($p = 0.32$) sensitivity—however, it had significant influence on point-wise mesopic ($p < 0.005$) and dark-adapted red ($p < 0.005$) sensitivity (Table S3).

In the combined linear mixed-effects models, only the point-wise RPEDC thickness and predominant drusen type exhibited statistically significant effects on sensitivity for all three types of testing (Table 2, Fig. 4). For mesopic testing, eyes with reticular drusen exhibited on average a lower sensitivity for all tests points of -1.53 SD (-3.67 dB considering the respective $SD_{overall}$ for all 49 test locations; cf., Table S2) as compared to eyes with cuticular drusen. Furthermore, for all three types of drusen, a point-wise thickening of the RPEDC by 1 SD ($SD_{overall}$ of 2.8 μm) would be associated with a point-wise sensitivity loss of -0.04 SD (i.e., -0.34 dB per 10 μm RPEDC thickening). For dark-adapted cyan testing, both eyes with reticular drusen (-1.91 SD; i.e., -5.73 dB) and eyes with soft drusen (-1.03 SD; i.e., -3.09 dB) exhibited on average lower sensitivity across all test locations as compared to eyes with cuticular drusen. Further, for all three types of drusen a point-wise RPEDC thickening by 1 SD would be associated with a decrease in point-wise dark-adapted cyan sensitivity by -0.01 SD (i.e., -0.11 dB per 10 μm RPEDC thickening). For dark-adapted red testing, both, eyes with reticular drusen (-1.18 SD; i.e., -2.83 dB) and eyes with soft drusen (-0.95 SD; i.e., -2.28 dB) exhibited on average lower sensitivity across all test locations as compared to eyes with cuticular drusen. Further, for all three types of drusen, a point-wise RPEDC thickening by 1 SD would be

Table 2 The table shows the effect estimates for the final models that included all variables with a significant effect in the separate models (cf. Table S3)

Parameter	Mesopic			Dark-adapted cyan			Dark-adapted red		
	Estimate	95% CI	p Value[a]	Estimate	95% CI	p Value[a]	Estimate	95% CI	p Value[a]
Intercept (cuticular drusen)	−0.35	−0.91 to 0.21	0.216	0.35	−0.08 to 0.78	0.112	−0.04	−0.55 to 0.47	0.89
Reticular drusen	−1.53	−2.36 to −0.70	**<0.001**	−1.91	−2.69 to −1.13	**<0.001**	−1.18	−2.03 to −0.32	**0.007**
Soft drusen	−0.24	−0.80 to 0.33	0.412	−1.03	−1.48 to −0.59	**<0.001**	−0.95	−1.54 to −0.36	**0.002**
Full ret. thickness	−0.03	−0.17 to 0.12	0.699	−0.07	−0.16 to 0.03	0.172	−0.06	−0.18 to 0.06	0.351
ONL thickness	0.01	−0.09 to 0.11	0.876	0.06	−0.05 to 0.17	0.254	−0.03	−0.12 to 0.06	0.544
IS + OS thickness	0.11	−0.08 to 0.31	0.257				0.11	−0.01 to 0.23	0.073
RPEDC thickness	−0.04	−0.06 to −0.02	**<0.001**	−0.01	−0.02 to −0.00	**0.003**	−0.03	−0.04 to −0.02	**<0.001**
Observations	2352			2352			2352		

[a]$p < 0.05$ Values were obtained from Wald tests

Please note, both the SD-OCT thickness data and slopes for the sensitivity represent Z-scores (respective number of standard deviation from the respective mean in normal eyes). For example for mesopic testing, eyes with reticular drusen (RDR) would exhibit overall thresholds that are lower by −1.53 SD or 3.67 dB (−1.53 × 2.4 dB, cf. Table S2) as compared to eyes with cuticular drusen (intercept). Bold values highlight p-values <0.05
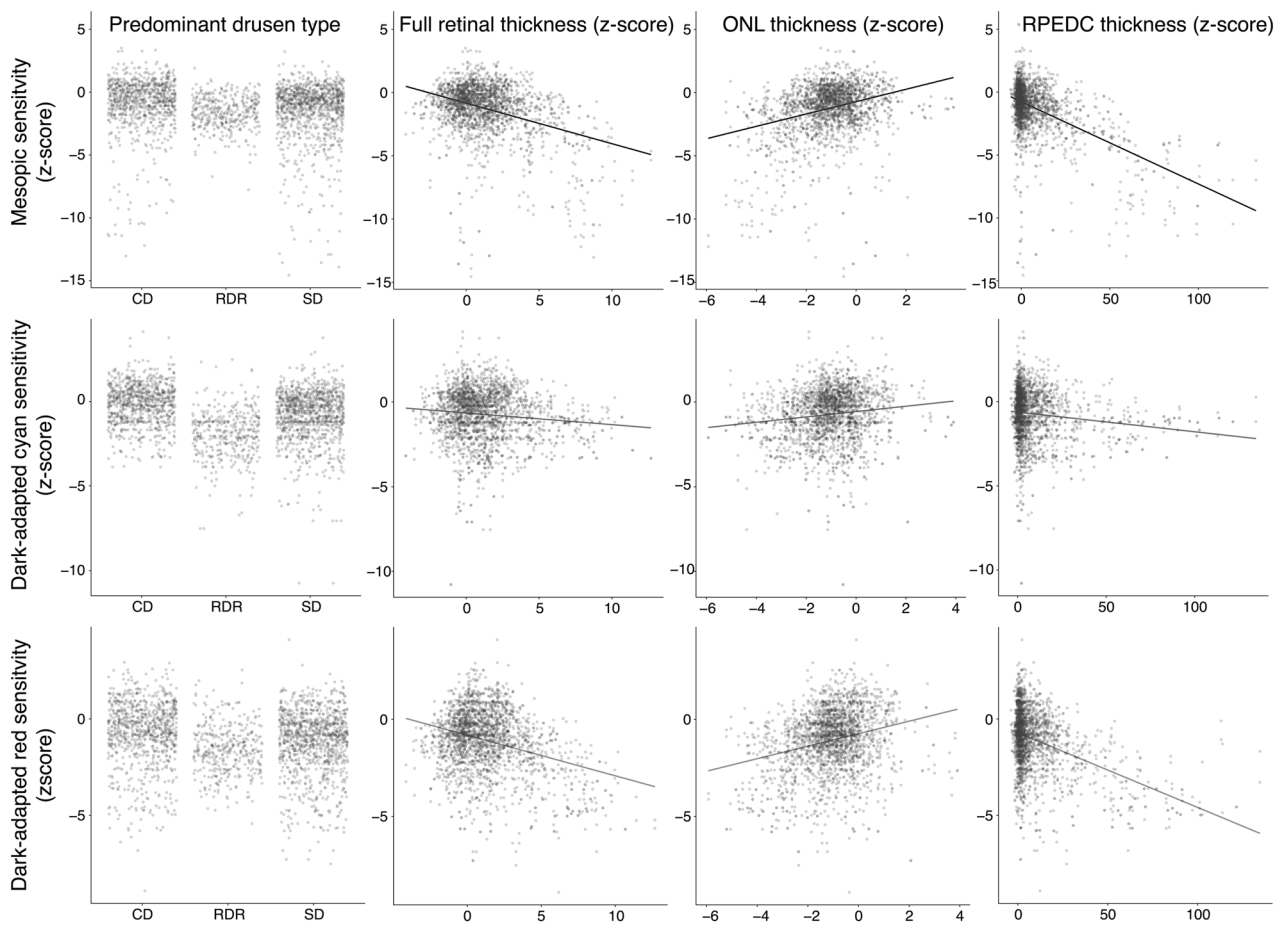
Fig. 4 Scatter plots for the mesopic (first row), dark-dapated cyan (second row), and dark-adapted red (third row) in dependence of the predominant drusen type (first column), full retinal thickness (second column), outer nuclear layer thickness (third column), and retinal pigment epithelium drusen complex thickness (fourth column). Since many data points obscured each other, the points were made semi-transparent. Further, the points of the first column (predominant drusen type) were spread along the x-axis to reduce overplotting. All data were plotted in terms of number of normative standard deviation from the normative mean (i.e., z-score). The largest differences in sensitivity in dependence of drusen type were observable for dark-adapted cyan testing. Yet, the steepest slopes in dependence of point-wise SD-OCT biomarkers were observable for mesopic and dark-adapted red testing

associated with a point-wise decrease in dark-adapted red sensitivity by -0.03 SD (i.e., -0.26 dB per 10 µm RPEDC thickening).

Discussion

This is the first study to demonstrate that the combination of mesopic and dark-adapted two-color FCP using the S-MAIA device allows for functional phenotyping in dependence of different drusen phenotypes in patients with intermediate AMD. The analysis was based on an innovative approach for structure-function correlation that included nonlinear image registration of FCP to SD-OCT data and acknowledged the precise size of stimuli (0.43° diameter). Retinotopic differences of the inter-individual variability of the normative SD-OCT and FCP data were considered.

The retest reliability as indicated by the short-term fluctuation was comparable to the retest reliability in normal eyes with the device [15]. While mesopic FCP yielded similar results among all subgroups, dark-adapted two-color FCP allowed for discrimination of functional deficits in dependence of the predominant drusen type. Previously, it was shown that mesopic threshold testing leads to "redundancy" in target detection (cone and rod function), resulting in ambiguous information and insensitivity in identifying minor degrees of isolated cone or rod dysfunction [43–45]. This could explain the similarity of the mesopic test results for all three subgroups. In contrast, two-color dark-adapted FCP allows for differential testing of rod function. Briefly, with the current stimulus luminance settings of the S-MAIA device, a cyan–red difference close to 0 dB (as observed at eccentricities of 5° and 7° in fully dark-adapted normal eyes) would be indicative of normal rod function [15]. Isolated rod dysfunction would result in a decrease of the cyan sensitivity as observed for the eyes with reticular drusen. Equal degrees of rod and cone dysfunction would lead to reduced cyan and red sensitivity; however, the cyan–red sensitivity difference would remain stable. This was observed in eyes with soft drusen. At fixation, isolated cone dysfunction would lead to a reduction of the red sensitivity, while the measured cyan sensitivity would not change significantly (due to the marked floor effects of the device for cyan testing). Thus, the results in eyes with cuticular drusen are indicative of isolated foveal cone dysfunction.

These results are in accordance with previous studies based on dark-adapted standard automated perimetry, rod-mediated dark adaptation, and electroretinography [8, 12, 14, 19, 29, 30]. Further, these results are in accordance with the histological observation that reticular drusen (subretinal drusenoid deposits) perentially localize to the perifovea—a location with high rod density [46]. It is conceivable that the marked differences in cone and rod function among eyes with cuticular drusen, soft drusen, and reticular drusen reflect differences of the underlying pathophysiology [26, 46]. Recent developments of novel agents that target photoreceptor classes specifically (such as visual cycle inhibitors, e.g., emixustat hydrochloride) highlight the need for differential testing of rod and cone function in the setting of AMD [47]. The results of the current study suggest that dark-adapted two-color FCP could allow to monitor both potential side effects and treatment effects of such pharmaceuticals more precisely as compared to mesopic FCP [45, 48, 49].

In terms of structural biomarkers, the ONL and IS + OS thicknesses might not have exhibited significant effect in the combined model either due to greater grading inaccuracy as compared to the RPEDC thickness or due to the underlying pathogenic mechanisms. With regard to grading inaccuracy, it must be noted that the inner boundary of the ONL was difficult to delineate due to the HFL [36, 50]. Especially in presence of drusen, the altered HFL orientation led to hypo- and hyperreflective segments complicating the automated segmentation and manual correction [36, 50]. The ELM, which served as boundary between the ONL and IS + OS, was sometimes interrupted or invisible further complicating delineation of these layers. As the absolute values for RPEDC thickness tend to be larger as compared to ONL and IS + OS thickness in eyes with drusen per se, it would be conceivable that any effects related to measurement inaccuracy relatively affect the quantification of the RPEDC thickness less as compared to the two latter layers. With regard to underlying pathogenic mechanisms, not only abnormal thinning but also paradox thickening of ONL has been described in proximity to drusen [36, 51]. Linear models do not account for such opposing effects. The results that IS + OS thickness exhibits a significant effect on mesopic and dark-adapted red sensitivity but not on dark-adapted cyan sensitivity is intriguing. This would imply that the IS + OS thickness reflects cone rather than rod function. However, this seems to be incompatible with the quasi-normal peripheral IS + OS configuration in diseases such as complete achromatopsia [52]. Further studies will be needed to reproduce this finding.

The estimates for mesopic sensitivity loss in dependence of RPEDC thickening in our data were surprisingly similar (-0.34 dB per 10 µm RPEDC thickening) as compared to a previous study by Wu et al. (-0.29 dB per 10 µm RPEDC thickening) despite of methodical differences [21]. The aforementioned study performed semi-automated segmentation using the DOCTRAP software (Duke University, Durham, NC, USA) instead of the Spectralis software and sector-wise instead of point-wise structure-function correlation [21]. The similarity of the results suggests that RPEDC thickness is a robust predictor of sensitivity.

However, soft drusen and reticular drusen regression (and consequently RPEDC thinning) have been previously described in natural history studies and were shown to be associated with subsequent outer retinal atrophy [20, 53, 54]. Thus, RPEDC thickness might not be optimal for longitudinal data analyses as it can both increase and decrease over time. In contrast, ONL thickness, which for the most part only decreases over time, could be potentially more meaningful in a longitudinal setting [36].

Several limitations of the study need to be considered. First, it was underpowered to explore possible interaction effects between RPEDC thickness and drusen type on sensitivity. Based on clinical observation, one could hypothesize that in eyes with reticular drusen a lesser amount of RPEDC thickening would result in relatively greater amount functional deficit as compared to eyes with soft drusen and cuticular drusen [8, 29, 30]. Second, the classification was purely based on multimodal imaging. No genetic testing was performed. Third, a radial grid instead of a rectilinear grid with uniform spacing was used in this study. The MD and cPSD in this study must be interpreted as spatially weighted averages due to the central condensation of test points [55]. Forth, the distribution of phakic versus pseudophakic eyes was not equal among all subgroups. In phakic eyes, lenticular absorption of short-wavelength light could potentially decrease the dark-adapted cyan sensitivity with increasing degrees of lens density (i.e., cataract) [56]. However, we observed the most severe decrease in dark-adapted cyan sensitivity in eyes with reticular drusen, the subgroup with the highest rate of pseudophakic eyes. Therefore, the estimated degree of rod dysfunction for eyes with reticular drusen as compared to the other types of drusen in this study is a rather conservative estimate.

In summary, the current study reports a systematic assessment of a recently introduced combined mesopic and dark-adapted two-color FCP device in the setting of intermediate AMD with various drusen phenotypes. It was demonstrated that dark-adapted two-color FCP (in contrast to mesopic FCP) provides differential information in dependence of drusen type. The results of the study may serve as basis for the application of dark-adapted two-color FCP as functional outcome measure in clinical studies in intermediate AMD.

Summary

What was known before

- Prompted by histological findings indicating that rod loss may exceed cone loss in eyes with age-related macular degeneration, previous studies have focused on probing rod function.

- These studies include dark-adapted perimetery and rod-mediated dark adaptation.
- Yet, all of the aforementioned functional tests are not fundus-controlled limiting the accuracy of structure-function correlation.

What this study adds

- The current study reports a systematic assessment of a recently introduced combined mesopic and dark-adapted two-color fundus-controlled perimetry (FCP) device in the setting of intermediate age-related macular degeneration (AMD) with various drusen phenotypes.
- It was demonstrated that dark-adapted two-color FCP provides differential information in dependence of drusen type, indicating predominant cone dysfunction in eyes with cuticular drusen and predominant rod dysfunction in eyes with reticular drusen.
- The results of the study may serve as basis for the application of dark-adapted two-color FCP as functional outcome measure in clinical studies in intermediate AMD.

Compliance with ethical standards

Conflict of interest CenterVue SpA, Padova, Italy has provided research material (S-MAIA) for the conduct of this study. CenterVue had no role in the design or conduct of the experiments.

References

1. Cheung LK, Eaton A. Age-related macular degeneration. Pharmacother J Hum Pharmacol Drug Ther. 2013;33:838–55.
2. Holz FG, Schmitz-Valckenberg S, Fleckenstein M. Recent developments in the treatment of age-related macular degeneration. J Clin Invest. 2014;124:1430–8.
3. Rasmussen A, Sander B. Long-term longitudinal study of patients treated with ranibizumab for neovascular age-related macular degeneration. Curr Opin Ophthalmol. 2014;25:158–63.
4. Schaal KB, Rosenfeld PJ, Gregori G, Yehoshua Z, Feuer WJ. Anatomic clinical trial endpoints for nonexudative age-related macular degeneration. Ophthalmology. 2016;123:1060–79.
5. Dimitrov PN, Robman LD, Varsamidis M, Aung KZ, Makeyeva GA, Guymer RH, et al. Visual function tests as potential biomarkers in age-related macular degeneration. Invest Ophthalmol Vis Sci. 2011;52:9457–69.

6. Curcio CA, Medeiros NE, Millican CL. Photoreceptor loss in age-related macular degeneration. Invest Ophthalmol Vis Sci. 1996;37:1236–49.

7. Owsley C, Jackson GR, Cideciyan AV, Huang Y, Fine SL, Ho AC, et al. Psychophysical evidence for rod vulnerability in age-related macular degeneration. Invest Ophthalmol Vis Sci. 2000;41:267–73.

8. Steinberg JS, Fitzke FW, Fimmers R, Fleckenstein M, Holz FG, Schmitz-Valckenberg S. Scotopic and photopic microperimetry in patients with reticular drusen and age-related macular degeneration. JAMA Ophthalmol. 2015;133:690–7.

9. Fraser RG, Tan R, Ayton LN, Caruso E, Guymer RH, Luu CD. Assessment of retinotopic rod photoreceptor function using a dark-adapted chromatic perimeter in intermediate age-related macular degeneration. Invest Ophthalmol Vis Sci. 2016;57:5436–42.

10. Owsley C, Jackson GR, White M, Feist R, Edwards D. Delays in rod-mediated dark adaptation in early age-related maculopathy. Ophthalmology. 2001;108:1196–202.

11. Sevilla MB, McGwin G, Lad EM, Clark M, Yuan EL, Farsiu S, et al. Relating retinal morphology and function in aging and early to intermediate age-related macular degeneration subjects. Am J Ophthalmol. 2016;165:65–77.

12. Flamendorf J, Agrón E, Wong W, Thompson D, Wiley H, Doss E, et al. Impairments in dark adaptation are associated with age-related macular degeneration severity and reticular pseudodrusen. Ophthalmology. 2015;122:2053–62.

13. Owsley C, McGwin G, Clark ME, Jackson GR, Callahan MA, Kline LB, et al. Delayed rod-mediated dark adaptation is a functional biomarker for incident early age-related macular degeneration. Ophthalmology. 2016;123:344–51.

14. Steinberg JS, Saßmannshausen M, Fleckenstein M, Fimmers R, Oishi A, Holz FG, et al. Correlation of partial outer retinal thickness with scotopic and mesopic fundus-controlled perimetry in patients with reticular drusen. Am J Ophthalmol. 2016;168:52–61.

15. Pfau M, Lindner M, Fleckenstein M, Finger RP, Rubin GS, Harmening WM, et al. Test-retest reliability of scotopic and mesopic fundus-controlled perimetry using a modified MAIA (Macular Integrity Assessment) in normal eyes. Ophthalmologica. 2017;237:42–54.

16. Pfau M, Lindner M, Muller PL, Birtel J, Finger RP, Harmening WM, et al. Effective dynamic range and retest reliability of dark-adapted two-color fundus-controlled perimetry in patients with macular diseases. Invest Ophthalmol Vis Sci. 2017;58:BIO158–67.

17. Steinberg JS, Sassmannshausen M, Pfau M, Fleckenstein M, Finger RP, Holz FG, et al. Evaluation of two systems for fundus-controlled scotopic and mesopic perimetry in eye with age-related macular degeneration. Transl Vis Sci Technol. 2017;6:7.

18. Pfau M, Lindner M, Steinberg JS, Thiele S, Brinkmann CK, Fleckenstein M. et al. Visual field indices and patterns of visual field deficits in mesopic and dark-adapted two-colour fundus-controlled perimetry in macular diseases. Br J Ophthalmol. 2018;102:1054-1059.

19. Wu Z, Ayton LN, Makeyeva G, Guymer RH, Luu CD. Impact of reticular pseudodrusen on microperimetry and multifocal electroretinography in intermediate age-related macular degeneration. Invest Ophthalmol Vis Sci. 2015;56:2100–6.

20. Wu Z, Ayton LN, Luu CD, Guymer RH. Microperimetry of nascent geographic atrophy in age-related macular degeneration. Invest Ophthalmol Vis Sci. 2015;56:115–21.

21. Wu Z, Cunefare D, Chiu E, Luu CD, Ayton LN, Toth CA, et al. Longitudinal associations between microstructural changes and microperimetry in the early stages of age-related macular degeneration. Invest Ophthalmol Vis Sci. 2016;57:3714.

22. Hartmann KI, Bartsch DU, Cheng L, Kim JS, Gomez ML, Klein H, et al. Scanning laser ophthalmoscope imaging stabilized microperimetry in dry age-related macular degeneration. Retina. 2011;31:1323–31.

23. Acton JH, Theodore Smith R, Hood DC, Greenstein VC. Relationship between retinal layer thickness and the visual field in early age-related macular degeneration. Invest Ophthalmol Vis Sci. 2012;53:7618–24.

24. Midena E, Vujosevic S, Convento E, Manfre' A, Cavarzeran F, Pilotto E. Microperimetry and fundus autofluorescence in patients with early age-related macular degeneration. Br J Ophthalmol. 2007;91:1499–503.

25. Vujosevic S, Pucci P, Casciano M, Longhin E, Convento E, Bini S. Long-term longitudinal modifications in mesopic microperimetry in early and intermediate age-related macular degeneration. Graefes Arch Clin Exp Ophthalmol. 2017;255:301–9.

26. Boon CJF, van de Ven JPH, Hoyng CB, den Hollander AI, Klevering BJ. Cuticular drusen: stars in the sky. Prog Retin Eye Res. 2013;37:90–113.

27. Cohen SY, Meunier I, Soubrane G, Glacet-Bernard A, Coscas GJ. Visual function and course of basal laminar drusen combined with vitelliform macular detachment. Br J Ophthalmol. 1994;78:437–40.

28. Finger RP, Charbel Issa P, Kellner U, Schmitz-Valckenberg S, Fleckenstein M, Scholl HP, et al. Spectral domain optical coherence tomography in adult-onset vitelliform macular dystrophy with cuticular drusen. Retina. 2010;30:1455–64.

29. Querques G, Massamba N, Srour M, Boulanger E, Georges A, Souied EH. Impact of reticular pseudodrusen on macular function. Retina. 2014;34:321–9.

30. Alten F, Heiduschka P, Clemens CR, Eter N. Multifocal electroretinography in eyes with reticular pseudodrusen. Invest Ophthalmol Vis Sci. 2012;53:6263–70.

31. Schmitz-Valckenberg S, Steinberg JS, Fleckenstein M, Visvalingam S, Brinkmann CK, Holz FG. Combined confocal scanning laser opthalmoscopy and spectral-domain optical coherence tomography imaging of reticular drusen associated with age-related macular degeneration. Ophthalmology. 2010;117:1169–76.

32. Auge J, Steinberg JS, Fleckenstein M, Holz FG, Schmitz-Valckenberg S. Retikuläre Drusen über die Zeit mittels SD-OCT. Ophthalmologe. 2014;111:765–71.

33. Ferris FL, Wilkinson CP, Bird A, Chakravarthy U, Chew E, Csaky K, et al. Clinical classification of age-related macular degeneration. Ophthalmology. 2013;120:844–51.

34. Cnaan A, NANM Laird, Slasor, Using P. the general linear mixed model to analyse unbalanced repeated measures and longitudinal data. Stat Med. 1997;16:2349–80.

35. Staurenghi G, Sadda S, Frcophth UC, Spaide RF, Nomenclature I, Tomography C, et al. Proposed lexicon for anatomic landmarks in normal posterior segment spectral-domain optical coherence tomography the IN OCT consensus. Ophthalmology. 2014;121:1572–8.

36. Sadigh S, Cideciyan AV, Sumaroka A, Huang WC, Luo X, Swider M, et al. Abnormal thickening as well as thinning of the photoreceptor layer in intermediate age-related macular degeneration. Invest Ophthalmol Vis Sci. 2013;54:1603–12.

37. Chiu SJ, Izatt JA, Connell RVO, Winter KP. Validated automatic segmentation of AMD pathology including drusen and geographic atrophy in SD-OCT images. Invest Ophthalmol Vis Sci. 2017;53:53–61.

38. Gliem M, Müller PL, Finger RP, McGuinness MB, Holz FG, Charbel Issa P. Quantitative fundus autofluorescence in early and intermediate age-related macular degeneration. JAMA Ophthalmol. 2016;134:817–24.

39. Pinheiro J, Bates D, DebRoy S, Sarkar D and R Core Team. nlme: Linear and Nonlinear Mixed Effects Models. R package version 3.1-137, (2018). https://CRAN.R-project.org/package=nlme.

40. Ferris FL, Kassoff A, Bresnick GH, Bailey I. New visual acuity charts for clinical research. Am J Ophthalmol. 1982;94:91–96.

41. Heijl A, Lindgren G, Olsson J. A package for the statistical analysis of visual fields. In: Greve EL, Heijl A, editors. Seventh international visual field symposium, Amsterdam, September 1986. Documenta Ophthalmologica Proceedings Series, vol 49. Springer, Dordrecht 1987. pp. 153-68.

42. Bebie H, Flammer J, Bebie T. The cumulative defect curve: Separation of local and diffuse components of visual field damage. Graefes Arch Clin Exp Ophthalmol. 1989;227:9–12.

43. Sloan LL. The threshold gradients of the rods and the cones in the dark-adapted and in the partially light-adapted eye. Am J Ophthalmol. 1950;33:1077–89.

44. Sloan LL. The Tubinger perimeter of Harms and Aulhorn. Recommended procedures and supplementary equipment. Arch Ophthalmol. 1971;86:612–22.

45. Simunovic MP, Moore AT, MacLaren RE. Selective automated perimetry under photopic, mesopic, and scotopic conditions: detection mechanisms and testing strategies. Transl Vis Sci Technol. 2016;5:10.

46. Curcio CA, Messinger JD, Sloan KR, McGwin G, Medeiros NE, Spaide RF. Subretinal drusenoid deposits in non-neovascular age-related macular degeneration: morphology, prevalence, topography, and biogenesis model. Retina. 2013;33:265–76.

47. Kubota R, Al-Fayoumi S, Mallikaarjun S, Patil S, Bavik C, Chandler JW. Phase 1, dose-ranging study of emixustat hydrochloride (Acu-4429), a novel visual cycle modulator, in healthy volunteers. Retina. 2014;34:603–9.

48. Zeavin BH, Wald G. Rod and cone vision in retinitis pigmentosa. Am J Ophthalmol. 1956;42:253–69.

49. Jacobson SG, Voigt WJ, Parel J-M, Apathy PP, Nghiem-Phu L, Myers SW, et al. Automated light- and dark-adapted perimetry for evaluating retinitis pigmentosa. Ophthalmology. 1986;93: 1604–11.

50. Lujan BJ, Roorda A, Knighton RW, Carroll J. Revealing Henle's fiber layer using spectral domain optical coherence tomography. Invest Ophthalmol Vis Sci. 2011;52:1486–92.

51. Sadigh S, Luo X, Cideciyan AV, Sumaroka A, Boxley SL, Hall LM, et al. Drusen and photoreceptor abnormalities in African-Americans with intermediate non-neovascular age-related macular degeneration. Curr Eye Res. 2015;40:398–406.

52. Greenberg JP, Sherman J, Zweifel SA, Chen RWS, Duncker T, Kohl S, et al. Spectral-domain optical coherence tomography staging and autofluorescence imaging in achromatopsia. JAMA Ophthalmol. 2014;132:437–45.

53. Spaide RF. Outer retinal atrophy after regression of subretinal drusenoid deposits as a newly recognized form of late age-related macular degeneration. Retina. 2013;33:1800–8.

54. Wu Z, Luu CD, Ayton LN, Goh JK, Lucci LM, Hubbard WC, et al. Optical coherence tomography-defined changes preceding the development of drusen-associated atrophy in age-related macular degeneration. Ophthalmology. 2014;121:2415–22.

55. Weleber RG, Smith TB, Peters D, Chegarnov EN, Gillespie SP, Francis PJ, et al. VFMA: topographic analysis of sensitivity data from full-field static perimetry. Transl Vis Sci Technol. 2015;4:14.

56. Charng J, Tan R, Luu CD, Sadigh S, Stambolian D, Guymer RH, et al. Imaging lenticular autofluorescence in older subjects. Invest Ophthalmol Vis Sci. 2017;58:4940–7.